DOI 10.1007/s10527-020-09999-x
Biomedical Engineering, Vol. 54, No. 3, September, 2020, pp. 179-183. Translated from Meditsinskaya Tekhnika, Vol. 54, No. 3, May-Jun., 2020, pp. 17-21.
Original article submitted July 11, 2019.

Investigation of the Lag Effect in X-Ray Flat-Panel Detector for Cone-Beam Computed Tomography

A. K. Avakyan*, I. L. Dergacheva, A. A. Elanchik, T. A. Krylova, T. K. Lobzhanidze, S. A. Polikhov, and V. P. Smirnov

The purpose of this work is to investigate the factors determining the magnitude and nature of the lag effect (residual signal) in the Varian PaxScan 4343CB flat-panel detector. Depending on the detector mode, typical value of residual signal is 1-2% after single exposed frame, increasing up to 3% after multiple exposures. The lag effect is the cause of up to 3.6% error of average flat-field signal measurement if used for averaging series of continuously exposed frames, which leads to incorrect assessment of X-ray attenuation coefficients. Spatial dependence of the lag effect is confirmed; the results of correction of projection images using spatially localized impulse response functions are demonstrated.

Introduction

Major tasks in radiotherapy are ensuring high dose delivery accuracy and minimizing dose loads applied to radiation-sensitive organs and tissues (critical organs and structures). These objectives require the shapes and positions of both the target and critical structures to be monitored throughout radiotherapy courses. The main monitoring device in the majority of remote radiotherapy systems is cone-beam computed tomography (CBCT), based on an X-ray source and an X-ray flat-panel detector (FPD). Such solutions were selected during development of the Onyx radiotherapy system by the Research Institute of Technical Physics and Automation under contract from the Russian Ministry of Education and Science and Rusatom Healthcare [1].

Lag causes the presence of a residual component of the initial signal in frames following the frame in which the initial signal was generated. The lag effect has the following explanations [2-6]:

– incomplete readout of the charge from capacitors;

– the effect of charge trapping with subsequent release in semiconductor photodiodes;

– scintillator afterglow;

– variation in the transfer characteristic of channels during irradiation.

Research Institute of Technical Physics and Automation, Moscow, Russia; E-mail: AKAvakyan@niitfa.ru
* To whom correspondence should be addressed.

If not properly controlled, the lag effect creates significant artifacts both in projection (2D) and tomographic (3D) images [7]. Compliance with technical specifications for the characteristics of X-ray images requires complex methods to be developed for measuring and compensating for lag. This report demonstrates the following main results:

– relationship between lag value and the number of frames read after exposure, the frame reading rate, binning, the intensity of the individual exposure, and multiple subsequent exposures;

– spatial nonuniformity of lag value across detector area;

– lag influence on the accuracy of measurement of the light field (the result of irradiation of the FPD in the absence of an object in the irradiation field) and, as a result, on measurement of the patient tissue X-ray attenuation coefficient.

An image correction algorithm was developed based on the results of investigation of lag properties. Correction of frames with consideration of spatial non-uniformity of lag was demonstrated.

Materials and Methods

Computed tomograph prototype. Studies were carried out on an experimental CBCT system consisting of a KRD-SM-150-1 X-ray apparatus (Spektr-AP, Russia)

and a Paxscan 4343CB detector (Varex, USA). This FPD model is fabricated using a structured cesium iodide (CsI) crystalline scintillator and a semiconductor support made of amorphous silicon (a-Si). Total area of the sensitive surface is 427 × 427 mm and the number of channels is 3072 long by 3072 wide with an option of analog binning. The readout rate is up to 25 fps. The magnitude of the digital signal in the output channel is measured in analog-to-digital units (ADU) in the range $0\text{-}2^{16}$.

The experiments in this study (unless otherwise indicated) used X-ray apparatus settings of 40 kV, 40 mA, 10 ms, frame rate 25 fps, and binning 3 × 3. All images were corrected by subtraction of the average dark frame recorded just before the experiment started. The relative lag value was expressed as percentage of the signal of the first exposed frame in the series.

Assessment of factors determining the magnitude of lag. A series of experimental measurements were performed to find out the relation of lag value to different factors:

– the number of frames read after exposure with a single pulse at readout rates of 5 and 15 fps (binning, 3 × 3);

– the number of frames read after exposure with a single pulse with binning of 1 × 1 and 3 × 3 (reading rate, 5 fps);

– single exposure signal magnitude (fixed tube voltage of 40 kV for 12 values of the product of tube current and pulse duration multiplication, giving a range of digital signals from 1000 to 54,000 ADU in the exposed frame);

– the spatial disposition of the detector channel (the assumption that lag shows spatial nonuniformity is based on the fact that the signal readout algorithm works from the center to the periphery of the detector matrix, resulting in time delays);

– the number of preceding exposed frames.

Lag correction algorithm. The real signal at the detector output Y is expressed by convolution of the true signal X with a multiexponential impulse response function (IRF) [2, 3]. The algorithm restores the true signal using the following system of equations:

$$\begin{cases} S_{n,k} = X_{k-1} + S_{n,k-1} \cdot e^{-a_n}; \\ X_k = Y_k - \sum_{n=1}^{N} b_n \cdot S_{n,k}, \end{cases} \quad (1)$$

where k is frame number, b_n and a_n are IRF parameters measured during calibration, N is the number of exponential components, and $S_{n,k}$ is the dynamic buffer variable accumulating data on previous exposures.

Preliminary studies were used to select the number of exponential components as $N = 4$, at which the total residual error of the experimental IRF approximation does not exceed 0.01%.

Effect of lag on adaptive radiotherapy implementation. Common procedure is division of X-ray image by light field image. The result of division determines the attenuation of radiation intensity passed through an object. The procedure also compensates for spatial nonuniformity of radiation field intensity and statistical differences in the transfer characteristics of FPD channels [8-11]. Execution of adaptive radiotherapy methods requires the electron density of tissues to be estimated on the basis of the coefficient of X-ray attenuation μ, which in turn is determined by an exponential attenuation law:

$$I = I_0 \cdot e^{-\mu x}. \quad (2)$$

In general case, coefficient μ depends on a number of factors, including the radiation spectrum, and as such is an integral value. Measurement of I_0 with sufficient accuracy requires averaging at least 128 light field frames.

The attenuation coefficient μ was measured using a Gammex Solid Water HE phantom at different substance thicknesses using two different methods for measuring the light field frame I_0. In the first, I_0 was obtained by averaging a sequence of sequentially recorded frames, while in the second I_0 was measured using an intermediate readout method in which the effect of lag was suppressed by reading 25 dark frames after each exposed frame [12].

The aim of these experiments was to evaluate the effects of the method used for obtaining the light field frame I_0 on determination of the attenuation coefficient μ in conditions in which the detector is presented. The magnitude of signal I attenuated by irradiated object was measured on an image obtained by exposure with a single X-ray pulse clearly not affected by lag. This measurement method provides for assessment of the effects of the averaged light field frame I_0 on the computation of μ independent of the projection conditions used for measurement of I. Tomographic projection acquisition mode (the detector is exposed to a continuous sequence of impulses, inducing lag) gives an assessment which can be regarded as valid on the assumption that lag is completely compensated by software processing.

X-Ray source parameters were: 70 kV, 15 mA, 10 ms; X-ray irradiation filters — 2 mm Al, 50 μm Cu, frame reading rate 25 fps, binning 3 × 3. A lead collimator with a window of diameter 2.5 mm was placed in front of the FPD to suppress the effect of radiation scattering and signals were measured in the projection of the collimator window.

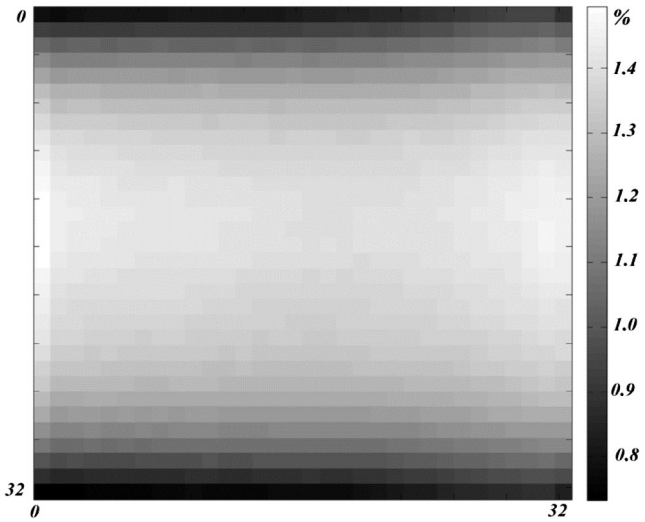

Fig. 1. Two-dimensional spatial distribution of relative lag in the first read frame after a single exposure.

Correction of lag with consideration of spatial nonuniformity. Lag was corrected, taking account of spatial nonuniformity, using an algorithm based on system of equations (1); during calibration, parameters b_n and a_n were measured individually for frame areas of size 32 pixels long by 32 pixels wide. At this size, deviations in the signal in a given channel from the average for the area were by no more than 8%; therefore, the IRFs of channels within this area were consistent. Increasing the size of the area made it impossible to achieve consistent IRF, while a reduction led to a sharp decrease in the measurement accuracy of parameters b_n and a_n because of the high noise level.

Signals were analyzed at 16 points along the central column of the last exposed frame and the first frame after exposure of a series of 100 sequential impulses. In the first case, IL was corrected using parameters b_n and a_n measured for local areas of the frame; in the second, using the averaged signal for the whole frame. Images were normalized to the light field.

Results

Factors determining the magnitude of lag. For readout frame rates of 15 and 5 fps, the relative magnitudes of lag in the first frame after exposure with a single pulse were 1.5% and 2.1%, respectively, with lag value dropping to 0.1% in both cases after six frames were read. For the 1 × 1 and 3 × 3 binning modes, relative lag values in the first frame after exposure with a single pulse were 0.6% and 2.1%, respectively.

Absolute lag value in the first frame read after a single exposure increased linearly with the increase of exposure signal. A similar linear relationship was also typical for subsequent frames read after a single exposure.

The spatial distribution of lag in the first frame read after a single exposure is shown in Fig. 1. In the direction of the columns, there was a decrease from 1.5% to 0.7% from center to periphery.

The magnitude of lag displayed a cumulative effect on exposure to continuous sequences of pulses (Table 1).

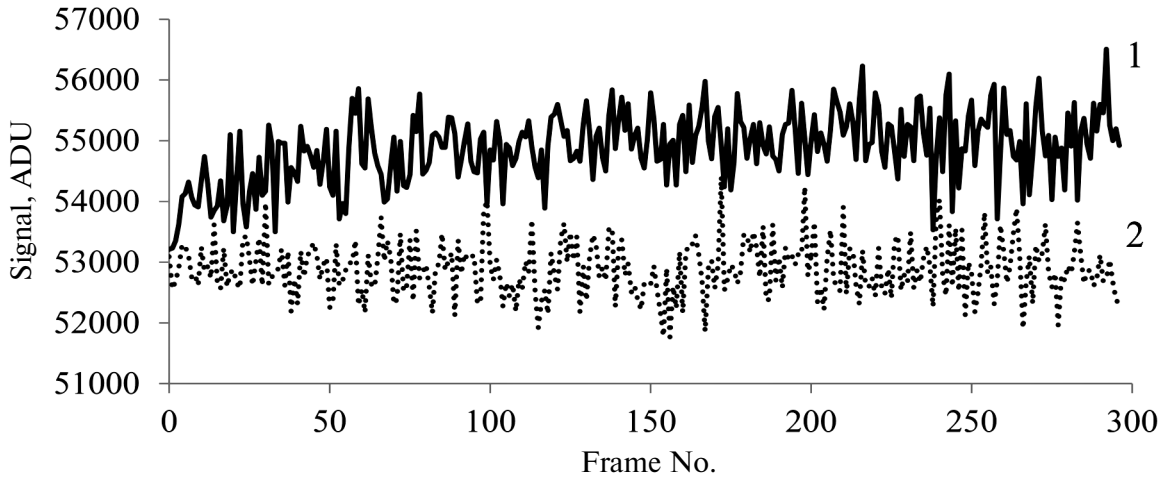

Fig. 2. Light field signal in the detector channel for sequential (1) and intermediate (2) readings.

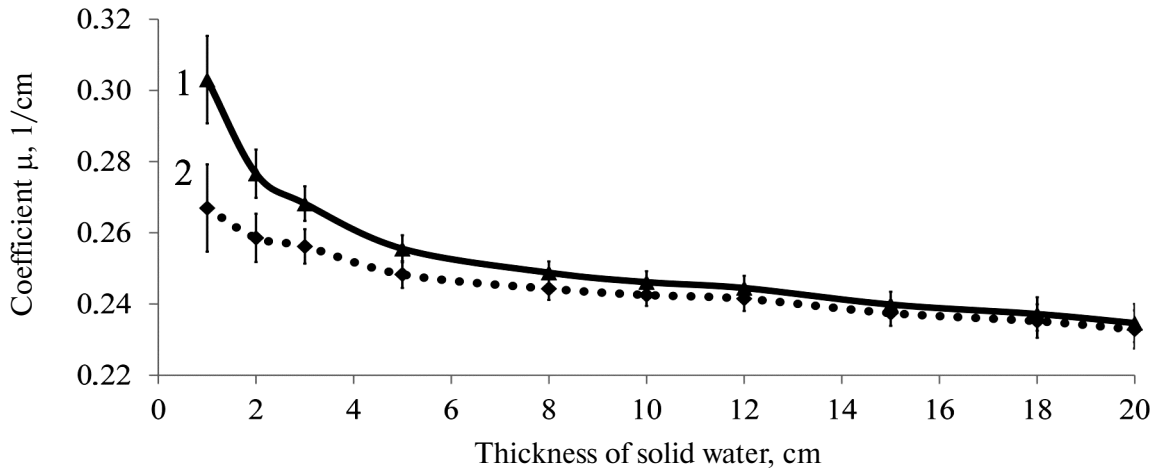

Fig. 3. X-Ray attenuation coefficient for sequential (1) and intermediate (2) readings.

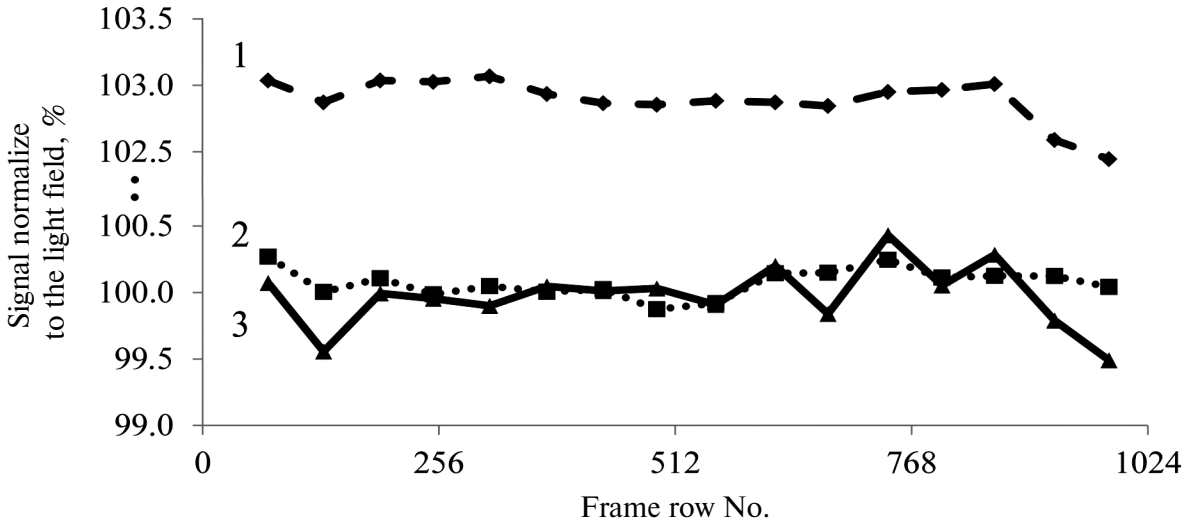

Fig. 4. Signal along the central column of the frame before and after correction of the lag: 1) initial with lag; 2) using location parameters; 3) using averaged parameters.

Lag in the case of light field normalization. The signals of the light field in the detector channel for intermediate and sequential readings are shown in Fig. 2. The cumulative lag effect was typical, leading to a measurement error of 3.2% in the mean value of the light field signal.

The relationship between the X-ray attenuation coefficient μ and the thickness of solid water is shown in Fig. 3. In theory, according to Eq. (2), the value of μ should be constant for any thickness of attenuating material. However, in practice, there is a 26% decrease in μ for sequential and a 12% decrease for intermediate readouts as the thickness of attenuating material increased from 1 to 20 cm. The effect can be explained by the simultaneous influences of two factors: the method for measuring the light field signal I_0 and hardening of the continuous spectrum of radiation on passage through the layer of attenuating material. Use of the intermediate readout method significantly decreased the error in determining μ at small (up to 8 cm) thicknesses of attenuating material. With further increases in thickness, the spectrum-hardening effect had a suppressive influence on assessment of μ.

Lag correction algorithm. Figure 4 shows the signal normalized to the light field in the 100th exposed frame in the series along the central columns of frame. The signal

TABLE 1. Lag in the First Frame after Exposure vs. Number of Previous Succeeding Exposed Frames (lag is expressed as percentage of the signal of the first exposed frame in the series)

Number of previous succeeding exposed frames	1	5	10	100	1000
Lag, %	1.0	1.6	1.9	2.7	3.1

is shown before lag correction , as well as after correction using local and averaged IRF parameters. Similar signal profiles were obtained for the first dark frame after the end of exposure, demonstrating a decrease in the normalized signal from 2.5-3.0% to 0%.

Conclusions

This article presents the results of experimental studies of the PaxScan 4343CB detector signal lag effect. Depending on capture mode, mean lag value was 1-2% of the single exposure signal and increased to 3.0-3.5% on multiple sequential exposures. A significant drop in lag occurred at the moment of succeeding frame readout. This article demonstrates the relationship between lag value and the frame readout rate, binning, and the intensities of single and multiple exposures. Spatial nonuniformity of lag was demonstrated: a decrease from 1.5% to 0.7% was seen in the direction of columns from the center to the periphery of the frame.

The study results provide grounds for using a multiexponential mathematical model of IRF in the lag correction algorithm. A comparison of results obtained by correction of images using spatially localized and frame-averaged IRF parameters is presented. In both cases, satisfactory results were obtained both for the last frame in dynamic exposure series (decrease in the normalized signal from 103% to 100%) and for the first dark frame after completion of exposure (a decrease in the normalized signal from 2.5-3.0% to 0%). Consideration of spatial nonuniformity in the correction algorithm did not provide any perceptible advantage.

The need to use the intermediate readout method in calibrating the average light field frame is confirmed. On sequential recording of light field frames, the averaging error reaches 3.2-3.6% due to the cumulative lag error effect, leading to an incorrect measurement of the X-ray attenuation coefficient of the patient's tissues. This result is particularly important in using adaptive radiotherapy methods.

Further development of this work will address evaluation of the effects of the lag correction method on the quality of 3D tomography reconstruction. Another necessary task is that of developing a method to take account of the spectral beam hardening effect on measurement of the tissue radiation attenuation coefficient.

This work was prepared within the framework of a contract between the Ministry of Education and Science of the Russian Federation and the Research Institute of Technical Physics and Automation under subsidy No. 14.582.21.0011 of October 3, 2017, "Creation and Progression to Clinical Trials of Prototype Import-Replacing Radiotherapy Systems based on Innovatory Equipment (6 MeV Accelerator and Cone-Beam Tomography)," unique identifier RFMEFI58217X0011.

REFERENCES

1. Rod'ko, I., et al., "Development of a radiotherapy system based on 6 MeV LINAC and Cone-Beam computer tomograph," Atomic Energy, **125,** No. 5, 292-296 (2019).
2. Starman, J., Lag Correction in Amorphous Silicon Flat-Panel X-Ray Computed Tomography, PhD Thesis, Stanford University (2011).
3. Di Sopra, L., Geometric Misalignment Calibration and Detector Lag Effect Artifact Correction in a Cone-Beam Flat Panel Micro-CT System for Small Animal Imaging, Master's Thesis, KTH, School of Technology and Health (2015).
4. Hsieh, J. "Analysis of the temporal response of computed tomography fluoroscopy," Med. Phys., **24,** No. 5, 665-675 (1997).
5. Rosas, S. F. P., Lag Correction for Cone-Beam CT: Master's Thesis, Tecnico Lisboa (2016).
6. Sato, H. et al., "Evaluation of image lag in a flat panel, detector equipped cardiovascular X-ray machine using a newly developed dynamic phantom," J. Appl. Clin. Med. Phys., **16,** No. 2, 366-375 (2015).
7. Cone Beam Computed Tomography, Shaw, C. C. (ed.), Taylor & Francis (2014), pp. 9-19.
8. Klyuev, V. V., Sosnin, F. R., and Aerts, V., X-Ray Technology. A Handbook [in Russian], Mashinostroenie, Moscow (1992).
9. Shafiei, S. A. and Hasanzadeh, H. "A simple calculation method for determination of equivalent square field," J. Med. Phys., **37,** No. 2, 107 (2012).
10. Avakyan, A. K., Zavestovskaya, I. N., Lobzhanidze, T. K., Polikhov, S. A., and Smirnov, V. P., "Digital flat panel detectors in medical imaging systems," Bull. Lebedev Phys. Inst., **45,** No. 11, 356-359 (2018).
11. Keuschnigg, P., et al., "Flat-field correction pipeline for a cone-beam computed tomography imaging device with independently movable source and detector," Med. Phys., **44,** No. 1, 132-142 (2017).
12. Lobzhanidze, T. K., Polikhov, S. A., and Avakyan, A. K., "A means of determining the transfer characteristics of pixels in flat panel detectors," RF Patent No. 2690105 (Application No. 2018137860; October 26, 2018) (2019).